

DTIC FILE COPY

GL-TR-90-0219

2

RESULTS OF A HIGH POWER OBLIQUE INCIDENCE  
HF IONOSPHERIC MODIFICATION EXPERIMENT

AD-A231 893

Gary S. Sales  
Ian G. Platt  
Yuming Huang

University of Lowell  
Center for Atmospheric Research  
450 Aiken Street  
Lowell, Massachusetts 01854

September 1990

Final Report  
(24 February 1987-15 June 1990)

Approved for public release; distribution unlimited.


GEOPHYSICS LABORATORY  
AIR FORCE SYSTEMS COMMAND  
UNITED STATES AIR FORCE  
HANSCOM AIR FORCE BASE, MASSACHUSETTS 01731-5000

DTIC  
ELECTE  
FEB 14 1991  
S B D

91 2 13 008

"This technical report has been reviewed and is approved for publication"

  
JOHN L. HECKSCHER  
Contract Manager

  
JOHN E. RASMUSSEN  
Branch Chief

FOR THE COMMANDER

  
ROBERT A. SKRIVANEK  
Division Director

This report has been reviewed by the ESD Public Affairs Office (PA) and is releasable to the National Technical Information Service (NTIS).

Qualified requestors may obtain additional copies from the Defense Technical Information Center. All others should apply to the National Technical Information Service.

If your address has changed, or if you wish to be removed from the mailing list, or if the addressee is no longer employed by your organization, please notify GL/IMA, Hanscom AFB, MA 01731. This will assist us in maintaining a current mailing list.

Do not return copies of this report unless contractual obligations or notices on a specific document require that it be returned.

REPORT DOCUMENTATION PAGE			Form Approved OMB No. 0704-0188	
<small>Public reporting burden for this collection of information is estimated to average 1 hour per response, including the time for reviewing instructions, searching existing data sources, gathering and maintaining the data needed, and completing and reviewing the collection of information, and comments regarding this burden estimate or any other aspect of this collection of information, including suggestions for reducing this burden, to Washington Headquarters Service, Directorate for Information Operations and Reports, 1215 Jefferson Davis Highway, Suite 1204, Arlington, VA 22202-4302, and to the Office of Management and Budget, Paperwork Reduction Project (0704-0188), Washington, DC 20503.</small>				
1. AGENCY USE ONLY (Leave blank)	2. REPORT DATE September 1990	3. REPORT TYPE AND DATES COVERED Final Report (24 Feb 1987-15 Jun 1990)		
4. TITLE AND SUBTITLE Results of a High Power Oblique Incidence HF Ionospheric Modification Experiment		5. FUNDING NUMBERS PE 61102F PR ILIR TA 7I WU AA  Contract F19628-87-K-0012		
6. AUTHOR(S) Gary S. Sales Ian G. Platt Yuming Huang				
7. PERFORMING ORGANIZATION NAME(S) AND ADDRESS(ES) University of Lowell Center for Atmospheric Research 450 Aiken Street Lowell, MA 01854		8. PERFORMING ORGANIZATION REPORT NUMBER  ULRF-466/CAR		
9. SPONSORING / MONITORING AGENCY NAME(S) AND ADDRESS(ES) Geophysics Laboratory Hanscom AFB, Massachusetts 01731-5000  Contract Manager: John Heckscher/LID		10. SPONSORING / MONITORING AGENCY REPORT NUMBER  GL-TR-90-0219		
11. SUPPLEMENTARY NOTES This research was supported by the Inhouse Laboratory Independent Research Fund.				
12a. DISTRIBUTION / AVAILABILITY STATEMENT Approved for public release; distribution unlimited.		12b. DISTRIBUTION CODE		
13. ABSTRACT (Maximum 200 words) From 25 January to 2 February 1990 an oblique ionospheric modification experiment using the VOA high power transmitter was carried out between Delano, CA and Shreveport, LA. A probe system, transmitting on a frequency close to that of the VOA heater signal was used to determine the effects of heating by observing the variation in its amplitude, angle of arrival and Doppler. A mid-point Digisonde was used for frequency management and as a HF radar for the detection of small scale heater-induced self-focussing irregularities. For this period VOA was not operating at its full power of 90 dBW so the experiment was largely considered as a fact finding exercise for future campaigns. As expected, data from both the probe system and Digisonde showed no unambiguous evidence as the heating cycle. Processed probe data for this period had significantly higher frequency spectral components than predicted and contaminate the spectra in the region near the heater cycle. These short period received signals are most likely due to naturally occurring structure in the ionosphere, such as multiple acoustic gravity waves, and the interference between the different propagation modes of the probe system. Digisonde drift data detected a large number of well defined large scale irregularities and gave a relatively smooth				
14. SUBJECT TERMS Oblique Ionospheric Modification; Ionospheric Structure; Ionospheric Irregularities; Acoustic Gravity Waves; AGW; VOA Heating; Ionospheric Heating			15. NUMBER OF PAGES 44	
			16. PRICE CODE	
17. SECURITY CLASSIFICATION OF REPORT Unclassified	18. SECURITY CLASSIFICATION OF THIS PAGE Unclassified	19. SECURITY CLASSIFICATION OF ABSTRACT Unclassified	20. LIMITATION OF ABSTRACT SAR	

### 13. ABSTRACT

spectrum at higher frequencies. The large amount of high frequency components in the Fourier spectrum highlights the need in future experiments to assess ionospheric conditions with a view to placing the heater cycle period in a clear region of the spectrum.



<b>Accession For</b>	
NTIS GRA&I	<input checked="" type="checkbox"/>
DTIC TAB	<input type="checkbox"/>
Unannounced	<input type="checkbox"/>
Justification	
By	
Distribution/	
Availability Codes	
Dist	Avail and/or Special
A-1	

## TABLE OF CONTENTS

	Page
1.0 INTRODUCTION	1
2.0 EXPERIMENTAL PROCEDURE	3
3.0 EQUIPMENT	6
3.1 Probe System	6
3.2 Digisonde 256	7
3.3 Oblique Sounder	7
4.0 EXAMPLES OF THE REAL TIME PROCESSED DATA	9
4.1 Probe Printout	9
4.2 VI Data	9
4.3 Sky Maps	13
5.0 POST PROCESSING DETAILS	14
5.1 Mode Separation	14
5.2 Fourier Analysis	15
6.0 EXAMPLES OF POST PROCESSED DATA	17
6.1 Amplitude	16
6.2 Elevation Angle	20
6.3 Skymap Data	28
6.4 Doppler Frequency	29

## TABLE OF CONTENTS (Continued)

	Page	
7.0 SUMMARY AND CONCLUSIONS	33	-
8.0 REFERENCES	36	-

## LIST OF FIGURES

Figure No.		Page
1	The MOF of the probe signal and the heater frequencies as a function of time for a) 31 January 1990, b) 2 February 1990	4
2	Example of real time probe data for the 31 January from 0633 to 0719 UT. The lower trace shows the variation in Doppler level (vertical scale) with a power scale. The upper trace is the elevation angle for the strongest spectral components.	10
3	The midpoint ionospheric parameters (foF2, hmF2, etc.) scaled from the midpoint vertical ionograms for a) 31 January 1990, b) 2 February 1990	11
4	Skymaps for 31 January 1990 from the period 0411 to 0501 UT. Under each individual plot: The left number gives UT, the center number (12) is the number of height gates (4) by the number of soundings (3) summed to obtain each sky map. The right number is the number of reflection sources.	12
5	Scatter plot of amplitude vs. elevation angles on 2 February for 0714 to 0808 UT. The elevation angles bounding the minimum, low/high and maximum regions are 8°, 17° and 24° respectively.	16
6	Amplitude versus time plot of the low and high ray for (a) 31 January during 0427 - 0622 UT and (b) 2 February during 0714 - 0807 UT	18

## LIST OF FIGURES (Continued)

Figure No.		Page
7	Fourier spectra of the low ray amplitude variation for two 24 minute periods on 31 January starting at a) 0536 UT, b) 0633 UT	19
8	Fourier spectra of the low ray amplitude variation for two 24 minute periods on 2 February starting at a) 0714 UT, b) 0726 UT	22
9	Simulation of the 5 min heater cycle amplitude by a sine wave injected into the data of 0714 UT on 2 February for a) 2 dB amplitude variation, b) 6 dB amplitude variation.	23
10	Elevation angle of the low and high rays as a function of time for the periods a) 0427 - 0623 UT on 31 January, b) 0714 - 0808 on 2 February.	24
11	Fourier spectra of the low ray elevation angle for the period 0427 - 0622 UT on 31 January	25
12	Fourier spectra of the low ray elevation angle for a subset (0557 - 0622 UT) of data in Figure 11 for 31 January 1990	26
13	Simulation of the 5 minute heater cycle change in elevation angle by using a sine wave injected into the data of 0427 UT on 31 January for a) a 2° elevation angle variation, b) a 0.6° elevation angle variation	27
14	Number of ionospheric reflection sources versus time for the periods a) 0320 - 0930 on 31 January, b) 0347 - 0920 on 2 February	30
15	Fourier spectra of the number of source data of the Digisonde for the period 0320 - 0930 on 31 January	31



## LIST OF FIGURES

Figure No.		Page
16	Doppler variation as a function of time for both the high and low ray for the period of 0714 - 0808 UT on 2 February	32

## 1.0 INTRODUCTION

During the period 25 January to 2 February 1990 an oblique ionospheric modification experiment was conducted between Delano, CA and Shreveport, LA. The high powered Voice of America (VOA) transmitter at Delano transmitted in an attempt to heat the F-region ionosphere over Albuquerque, NM some 1200 km down range. A low power probe also transmitting at Delano on a frequency very close to that of the VOA frequency, and thereby producing a similar propagation path, was received at Shreveport approximately 2400 km down range at a bearing of  $91.3^\circ$  T. Since the probe signal will travel through the region most affected by the high powered VOA transmission, it can be used to determine the effect it has on ionospheric modification (see *Sales and Platt, 1989*).

From theory, it is expected that the high powered radio wave from VOA will modify the ionosphere in two ways. Firstly, near the F-region reflection point of the propagation path, electrostatic instabilities will be generated and a large heater-induced region of electron density depletion formed (*Gurevich, 1990 private communication*). The expected heated region would typically be some 20 km in height and 100 km in width, with a depletion in electron density of  $\sim 5\%$ . The precise values of the depletions parameters depend on the VOA radiated power pattern and ionospheric conditions.

Secondly, lower down in the ionosphere, self focusing of the beam may cause already existing irregularities to be enhanced (*Gurevich, 1978*). Since the electric field threshold for these instabilities is only  $\sim 1$  mV/m, and the VOA signal in this area is estimated to be several hundred mV/m, a large number of these irregularities are likely to be produced. Soviet experiments have indicated that the combined effect of these regions can cause significant deviations to be observed in the probe signals Doppler, angle of arrival and amplitude (*Bochkarev et al., 1982*).

Due to the fact that the VOA facility was not operating at full power during the time of this experiment (only one of the transmitters was

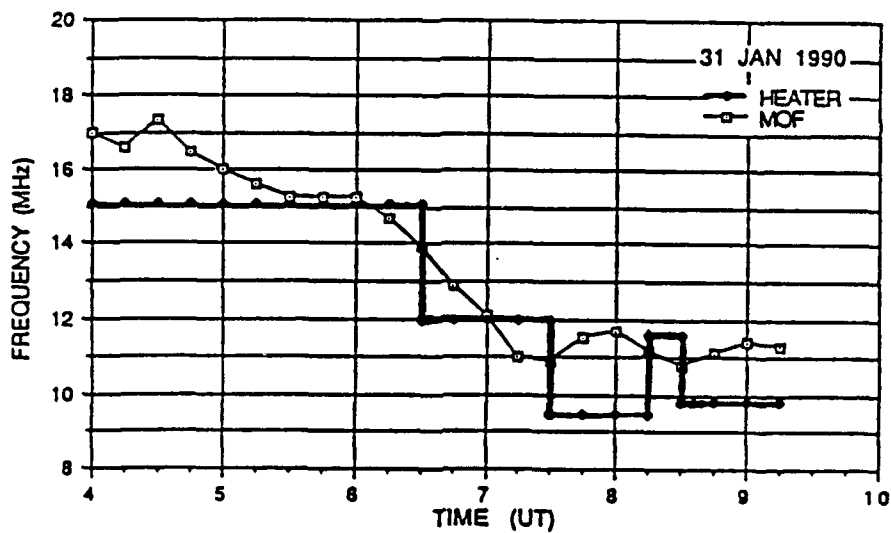
operational providing only 375 kW) the test was considered to be a fact finding mission to determine: 1) the practicality and reliability of the operational set up (e.g. frequency management, antenna spacing, software, etc.), 2) the accuracy of the probe system in determining the Doppler, amplitude and angle of arrival information, 3) the difficulties encountered in post processing real data such as determining, high and low rays, possible saturation conditions of the probe receivers, etc., 4) the effect that natural ionospheric fluctuations had on the experiment.

## 2.0 EXPERIMENTAL PROCEDURE

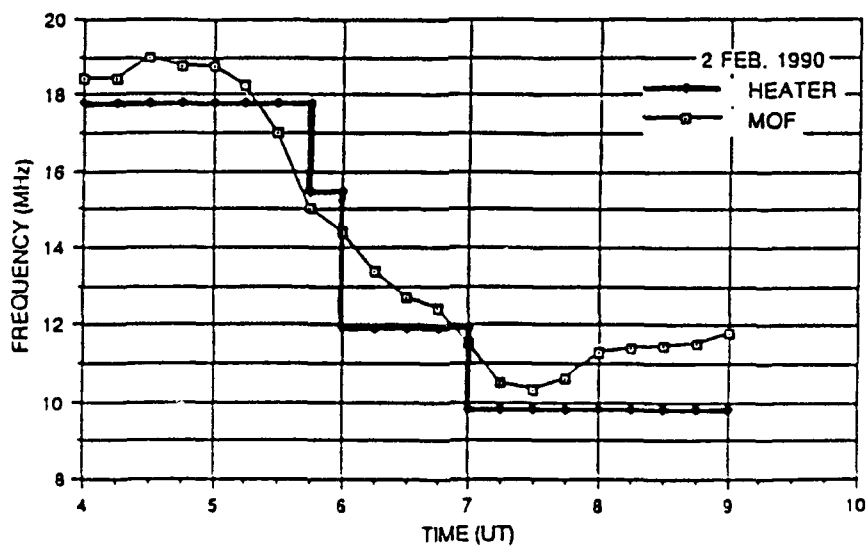
The experiment was conducted over the period of 25 January 1990 to 2 February 1990 beginning at 0400 UT of each night and lasted for 5 hours. Nighttime was chosen for the experiment since there is no D-region absorption to decrease the power deposited in the upper ionosphere and the low critical frequency of the maximum layer ( $f_oF_2$ ) means that a lower operating frequency value could be used to place the signal closer to the layer peak. The second point is important since the heating effect is increased with both a decrease in the operating frequency and closer proximity to the Maximum Usable Frequency (MUF).

One of the major problems with the experiment was the lack of adequate frequency selection for the VOA transmitter. The optimal position for the skip is some 50-300 km up range from the receiver site (*Sales and Platt, 1989*) and this requires the operating frequency to be close to (and below) the MUF. Since the ionosphere was changing during the night a number of VOA frequency changes were necessary in an attempt to maintain this optimum condition. The VOA can only operate at a number of discrete frequency bands around ~ 6, 9, 11, 13, 15, 17 MHz and this means that for much of the night it is not transmitting at the optimum frequency value for heating. The operational procedure thus consisted of picking the operating frequency below the calculated MUF and waiting for the ionosphere to decay enough so that the MUF value passed through it. Just before this happens is the best time to look for the heating effect. Figures 1a and 1b show the chosen VOA operating frequencies plotted with the Maximum Observed Frequency (MOF) for the nights of 31 January and 2 February respectively.

The chirp sounder can provide the MOF for the path, but as already pointed out one of the important parameters in maximizing the observation of the heated portion of the ionosphere, is the distance of the skip from the receiver site. To determine this, ray tracing is necessary and this in turn requires knowledge of the ionospheric parameters near the midpoint of the path at Kirtland. The major ionospheric parameters determined from the scaled ionogram were observed and calibrated by the Digisonde and then



a)



b)

Figure 1. The MOF of the probe signal and the heater frequencies as a function of time for a) 31 January 1990, b) 2 February 1990

telephoned to Shreveport where they were included in a simple quasi-parabolic analytic ray tracing program to indicate the position of the skip. A decision on adjustment of the VOA frequency was then made for best placement of the skip. The ray tracing was also used as a real time check of the elevation angle determined by the probe system. Both the selected operating frequency and elevation steer angle are telephoned to Delano.

## 3.0 EQUIPMENT

### 3.1 Probe System

The probe system consisted of a 500 W CW transmitter at Delano, CA and three RACAL receivers at Shreveport, LA. The system is designed so that the probe transmission operates on a frequency just below (30-60 kHz) that of the VOA heater signal so that it passes through the heater-induced depletion region. The probe and VOA transmission frequencies are sufficiently different however, to ensure that the high power VOA signal does not interfere with the probe receivers.

The three antennas (one for each receiver) are placed in two line arrays to form an "L" shaped configuration, each line capable of acting as an interferometer, to measure elevation and azimuth of the received signal. One line array of the configuration consisting of two antennas ~ 100m apart, is parallel to the great circle path between Delano and Shreveport and is therefore most sensitive to elevation angle measurements. The other line of the array consisting of two antennas ~ 30m apart, is perpendicular to the first and is therefore most sensitive to azimuth angle measurements. The antenna that is common to both is used as a reference antenna.

The Coherent Integration Time (CIT) of the probe system is 23.3 seconds, in which time it collects 4096 complex points of data (In-phase and Quadrature components) from each of the three antennas. When this is complete a Fourier analysis is done in real time to provide 4090 ( $\pm 100$  Hz) Doppler spectrum lines of which the 400 ( $\pm 9.7$  Hz) centered around 0 Hz are selected for post processing. Only 400 ( $\pm 9.7$  Hz) Doppler lines of the total spectrum need be retained for post processing since this is sufficient to observe the expected natural fluctuations of the ionosphere as well as those produced by the heating. For the real time display the peak amplitude of this Doppler spectra is chosen and processed to give its elevation angle (only the elevation pair of antennas are processed in real time). The Doppler spectra, peak amplitudes of these spectra and their associated elevation angles are then displayed.

The received probe signal is post processed by Fourier analyzing sections comprised of 64 of these spectra, to identify the variations in amplitude and angle of arrival caused by the heater cycle.

### 3.2 Digisonde 256

A Digisonde 256 was installed at Kirtland, NM (the mid-point of the propagation path) to produce Vertical Incidence (VI) ionograms every 15 minutes. The resulting ionograms were scaled to provide the necessary ionospheric parameters, such as foF2, hmF2 and ymF2 to aid in the role of frequency management.

By selecting its drift mode of operation the Digisonde was also used, in between the time taken for the VI soundings, as a HF radar to determine the existence of the heater induced self-focussing irregularities. Irregularities in the ionosphere are detected as reflection sources over a large range of zenith angles, where the position of each source is determined from the phase difference of the same spectral line on the signal received by each of the four Digisonde antennas. In order to reduce the effect of noise on the skymaps and thus pick only those reflection sources resulting from relatively strong irregularity structures, only the strongest spectral lines are processed and plotted.

Details of the Digisondes drift mode of operation can be obtained from *Dozois*, (1983).

### 3.3 Oblique Sounder

A swept frequency oblique sounder operating over the frequency range of 6-30 MHz was used over the 2400 km Delano-Shreveport path to provide an independent measure of the MOF. The oblique ionograms were made every 15 minutes and from this data an extrapolation made to estimate the skip distance for the heater/probe operating frequency. Since the oblique sounding system does not give values for ionospheric parameters at the mid point of the propagation path it cannot be accurately used for the



determination of elevation angles or for ERP calculations (described in section 7.0), that require ray tracing.

## 4.0 EXAMPLES OF THE REAL TIME PROCESSED DATA

### 4.1 Probe Printout

An example of the real time printout of data processed from the probe receiver for the period 0633-0719 UT on 31 January is shown in Figure 2. The lower section of this figure shows the variation in Doppler (vertical scale) with time (horizontal scale) for the strongest spectral components. The upper portion of the figure is a plot of the elevation angle (vertical scale) with time for several spectral components. Note that time increases from right to left on these plots, and the far left of the plot is where the probe transmission frequency goes through the MUF.

Clearly noticeable in the Doppler plot are two modes, most likely corresponding to the low ray and high ray. These modes merge as the operating frequency approaches the MUF. The upper plot of Figure 2 shows that the two modes are considerably different in elevation angle with the low ray varying between 18-20° and the high ray varying between 22-30°. As expected the elevation angle of both rays also become similar near the MUF.

Another noteworthy point in the Doppler spectrum is an offset from 0Hz of the mean received power in the spectrum, most noticeable where the two traces merge near the MUF. This effect is most likely due to the bulk vertical motion of the ionosphere and for the approximate -0.6Hz Doppler frequency value near the MUF corresponds to the F-layer peak moving upwards with a velocity of 23 m/s. From Figure 3a, described in the following section, it can be seen that during this period the F-peak was indeed moving upwards.

### 4.2 VI Data

The midpoint VI ionograms are automatically scaled and inverted to produce the significant ionospheric parameters every 15 minutes. Figures 3a and 3b show a plot of the resultant parameters for part of each night on 31 January and 2 February respectively. On each plot is shown the

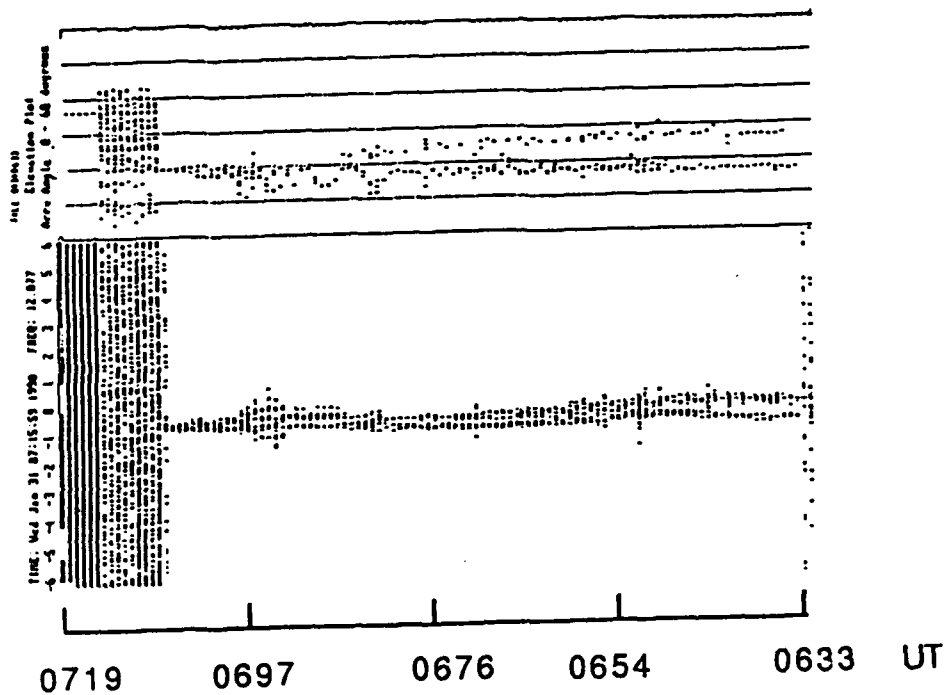
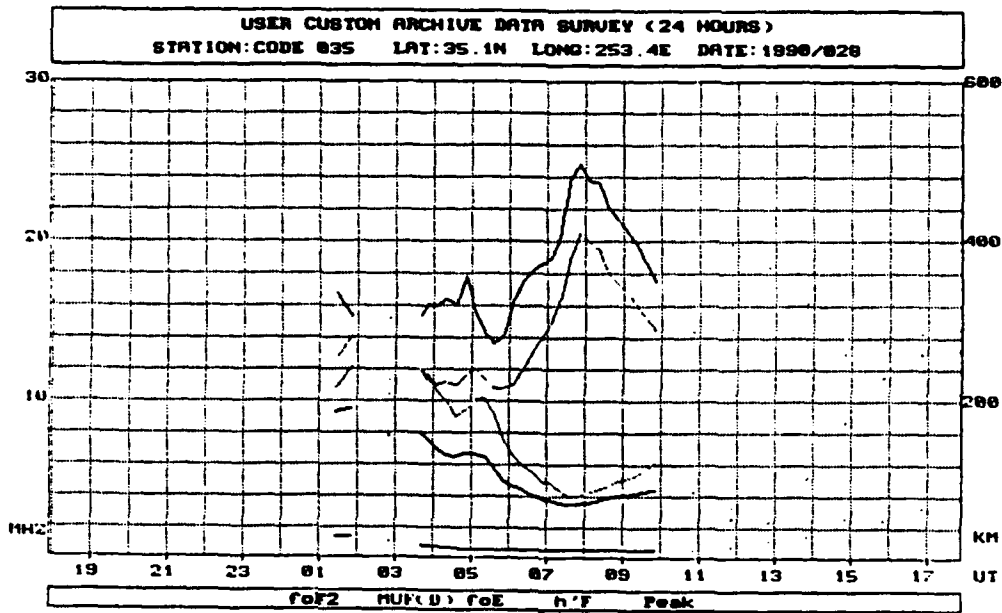
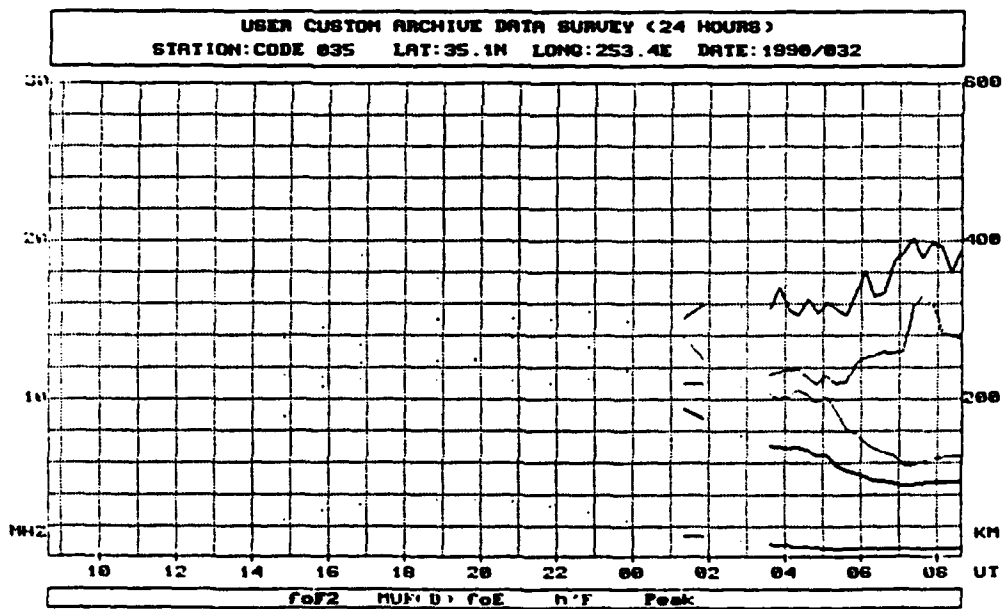


Figure 2. Example of the real time probe data for the 31 January from 0633 to 0719 UT. The lower trace shows the variation in Doppler level (vertical scale) with a power scale. The upper trace is the elevation angle for the strongest spectral components.



a)



b)

Figure 3. The midpoint ionospheric parameters (foF2, hmF2, etc.) scaled from the midpoint vertical ionograms for a) 31 January 1990, b) 2 February 1990

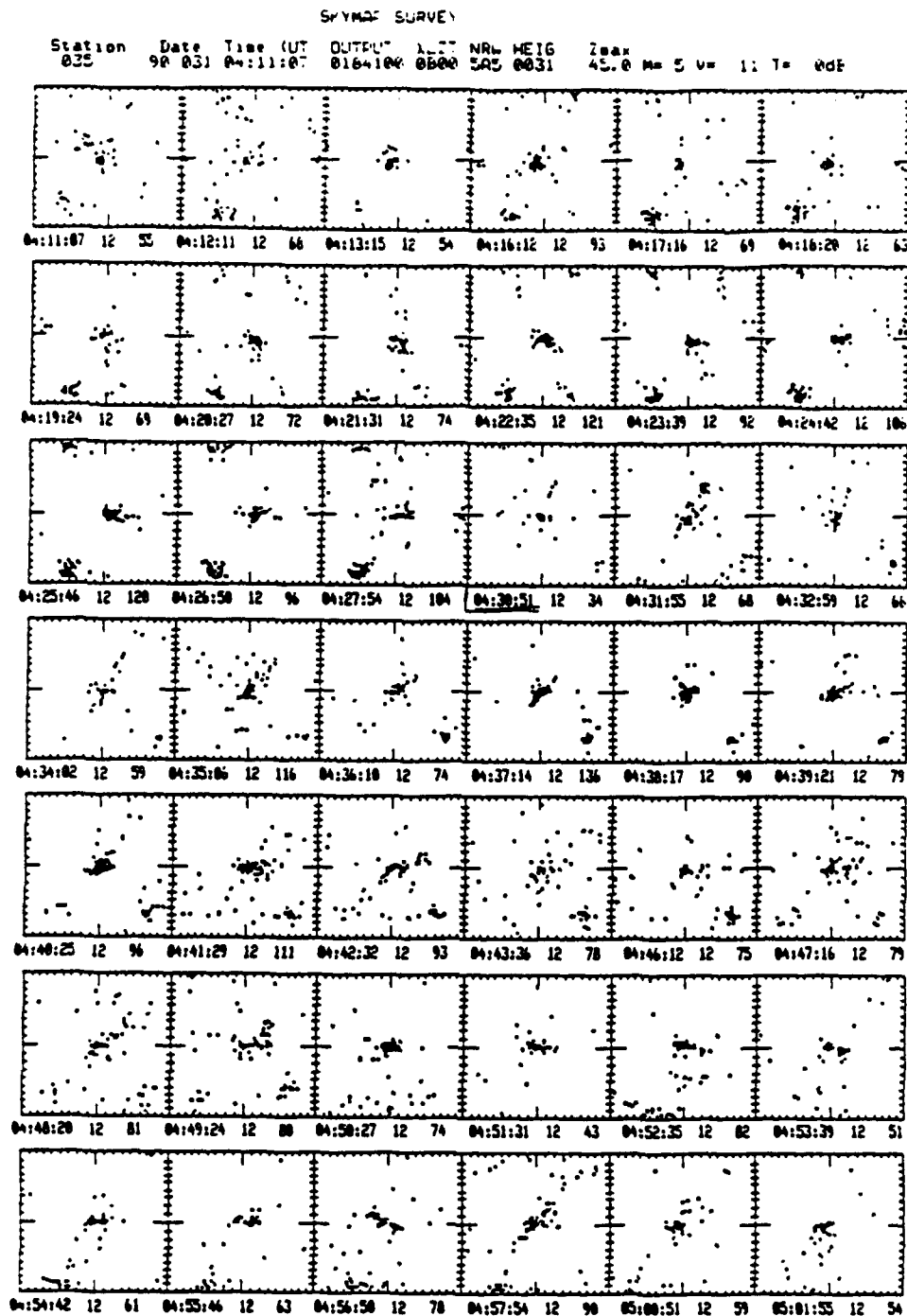


Figure 4. Skymaps for 31 January 1990 from the period 0411 to 0501 UT. Under each individual plot: The left number gives UT, the center number (12) is the number of height gates (4) by the number of soundings (3) summed to obtain each sky map. The right number is the number of reflection sources.

plasma frequency of the F-peak ( $f_oF_2$ ), the calculated MUF, the modelled plasma frequency of the E-layer ( $f_oE$ ) which is not significant in these cases, the height of the base of the F-layer ( $h'F$ ) and the height of the peak of the F-layer. The true height of the F-peak is obtained by an automatic inversion of the ionogram, while the true height of the base of this layer is taken to be the lowest virtual height value scaled from the F-layer trace.

#### 4.3 Sky Maps

An example of the Digisonde output of ionospheric parameters suitable for frequency management and post processing requirements has already been given in Figure 3. As mentioned before however, the heated region is expected to produce irregularities that can be observed by the Digisonde in its HF radar (drift) mode. An example of skymap data is shown in Figure 4. This figure comprises 42 skymaps from 0502 to 0551 UT on 31 January 1990. Each point on the plot indicates the position (zenith and azimuth) of an ordinary ray reflection point for a particular group path. The time between individual skymaps is 64 seconds, with each being constructed from the sum of 12 sounding sub cases. The middle of the map corresponds to the overhead position while the edges of the map correspond to a zenith of  $45^\circ$ . This plot is for the ordinary ray only with four height gates at 370, 380, 415 and 420 km (frequency = 6.3 MHz). The number and position of sources in each skymap is the important factor in determining the generation of small scale irregularities produced by the heater. Though the 64 second time between each plot is normally sufficient to recognize the 5 minute growth decay cycle of any heater induced irregularities, the period between each sky map can be reduced to 20 seconds if this becomes necessary.

## 5.0 POST PROCESSING

### 5.1 Mode Separation

One of the major problems in processing angle of arrival data was the identification of the high and low rays (and any other modes that may be present). The most robust and accurate method to achieve this identification consists of tackling the problem in two steps. Firstly, a plot is made of the elevation angle for all Doppler lines (up to a maximum of 8 Doppler lines) that fall above a power threshold (i.e. all points whose power is greater than 26 dB below the maximum). On the resulting elevation angle versus power scatter plot, a second threshold value is chosen for the power (below which no values are further considered) by choosing a noise floor for the plot. Secondly, three elevation angle lines are then marked to partition off the major density areas of the scatter plots. The first line represents the minimum elevation angle that will be considered, the second divides the density regions between low ray and high ray (this line is chosen so that two clear and well separated peaks can be distinguished) while the third line represents the maximum elevation angle that will be considered. The two outside maximum and minimum lines are used to eliminate elevation angle values that are clearly unreasonable. The low ray is then determined to be that ray which falls within the lower bounded area of the scatter plot (area A on Figure 5) while the high ray is that ray which falls within the upper bounded area (area B on Figure 5). If more than one Doppler line passes the test to be called either a high ray or low ray for one sample time, the elevation angle chosen is the power weighted mean.

An example of high and low ray elevation angles determined by this method are shown in Figure 10 as a function of time. This example is for the period 0714-0808 on 2 February 1990 and will be discussed more fully in the next section. For this case the lower power threshold is chosen to be 300.0, the lower elevation angle line is  $8^\circ$ , the line separating low and high ray is  $17^\circ$  and the maximum elevation line is  $24^\circ$ .

## 5.2 Fourier Analysis

A Fourier spectral analysis was done on the amplitude data to look for the five minute heater signal which would show at the 3.3 mHz position in the spectrum. For this analysis only the amplitude of the low ray was used. Discontinuities in the data imposed by gain and frequency changes cannot be included in the data set used for Fourier processing. The data is thus broken up into 24 minute strips each of which does not contain any of these discontinuities. For a 5 hour campaign this gives 12 individual spectra. To smooth these spectra additional time periods overlapping the last and first 12 minutes of adjacent strips are also processed.



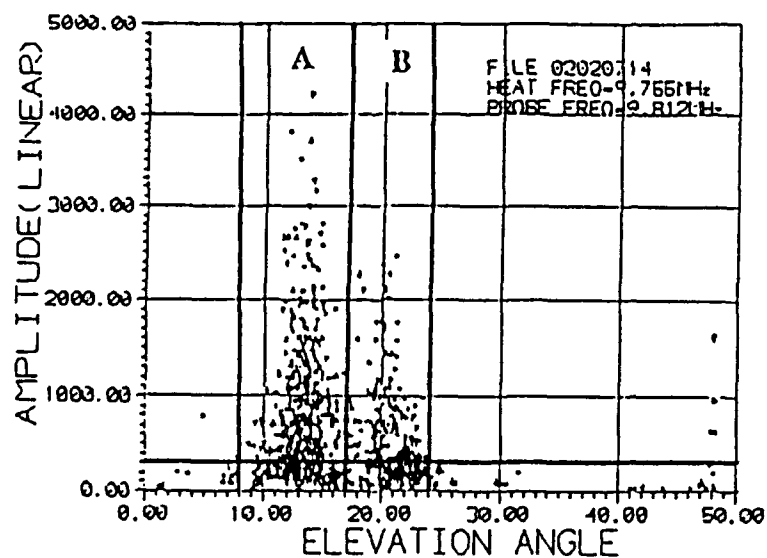


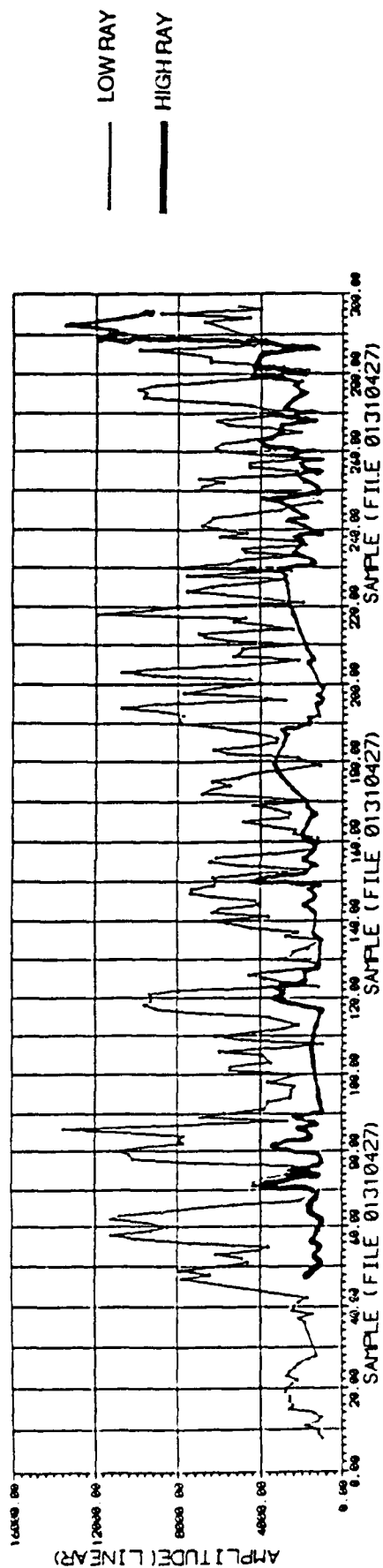
Figure 5. Scatter plot of amplitude versus elevation angle on 2 February for 0714 to 0808 UT. The elevation angles bounding the minimum, low/high and maximum regions are 8°, 17° and 24° respectively.

## 6.0 EXAMPLES OF POST PROCESSED DATA

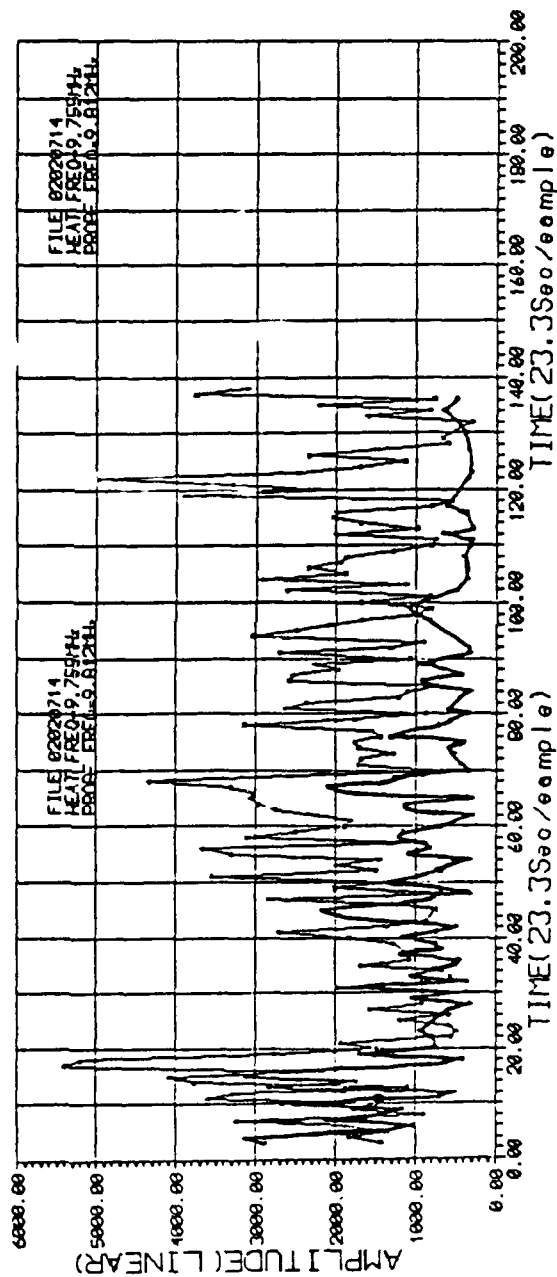
### 6.1 Amplitude

Figures 6a and 6b are plots of the received signal amplitude on the reference antenna for the low ray over the testing period for 31 January on 0427 - 0622 and 2 February on 0714 - 0807 UT respectively. Particularly noticeable in both figures is the deep, short period fading usually impressed upon a less intense and much larger (>10 minute) period fading. The longer period fading can easily be explained by the effect that large scale ionospheric structures, such as Atmospheric Gravity Waves (AGWs), have on a single propagation mode. The short period fading is seen to be considerable even over one CIT of 23.3 seconds and though it could be purely the result of the variation imposed upon a single propagation mode passing through a highly structured ionosphere (resulting from the effect of many AGW's for example), a more likely explanation is that it is caused by interference between different wave modes: primarily interference between O and X modes and interference between micro-modes. Micro-modes occur due to comparatively small geometric differences in ray paths resulting from multiple reflection points from ionospheric structures such as AGW's. The resulting modes may have similar Doppler and angles of arrival at the receiver, and interfere to cause rapid fading. O and X modes are not separable on the raw data plots indicating that their Doppler and elevation angles are nearly the same, and thus their resulting interference will also cause fading.

Figures 7a and 7b are two 24 minute long Fourier spectra starting at 0536 UT and 0633 UT respectively, on January 31. Comparing these times with Figure 1a it can be seen that both these periods correspond to times when the heater frequency was close to the MUF, thus optimizing the heating effect. Both figures display maximum power near the low frequency end of the spectra that gradually falls off as the frequency increases. It is likely that a dominant AGW (of period > 10 minutes) is responsible for the very low frequency power, while multiple AGW interference effects (causing 2 - 10

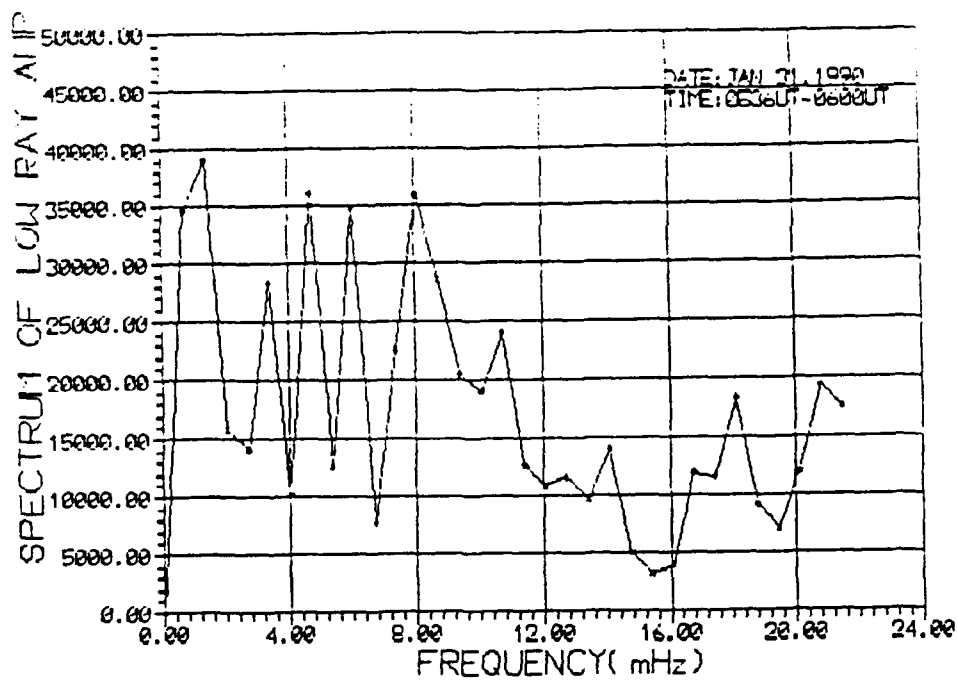


a)

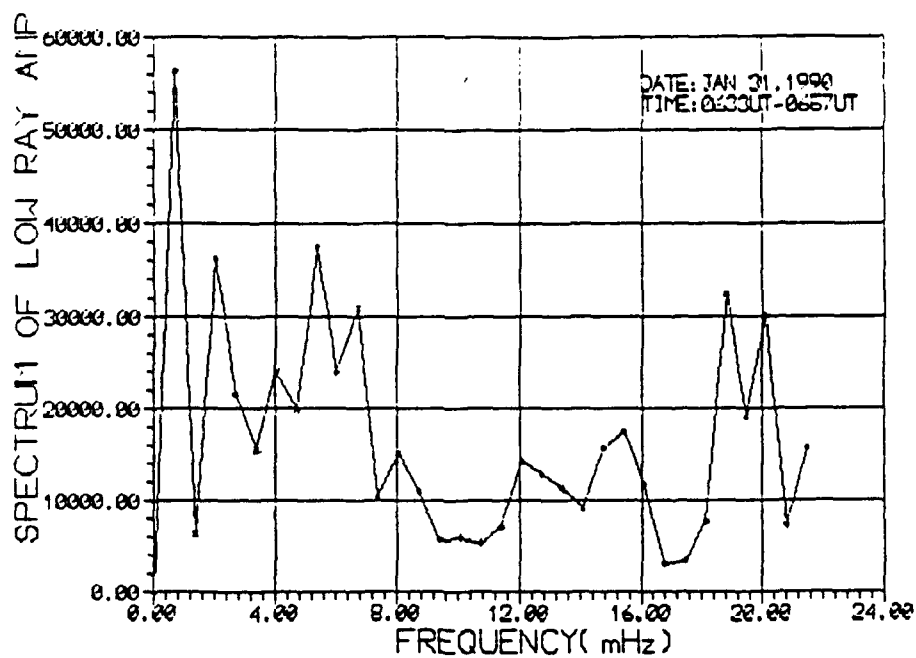


b)

Figure 6. Amplitude versus time plot of the low ray for a) 32 Jan. during 0427-0622 UT, and b) 2 Feb. during 0714-0807 UT



a)



b)

Figure 7. Fourier spectra of the low ray amplitude variation for two 24 minute periods on 31 January starting at a) 0536 UT, b) 0633 UT

minute periods) are responsible for the higher frequency power observed. The spectra for the February 2 data are shown in Figure 8. Here 8a for the time period starting at 0714 UT displays similar characteristics to that of the January 31 data, while Figure 8b starting at 0726 UT gives a flatter almost white noise like spectra.

The large amount of variability of the spectra in the region of the heater cycle (3.3 mHz) means that the heating effect will have to deposit a substantial amount of power into the spectra before it is clearly recognizable over the background noise. Figure 9a shows the result of a 5 minute period (3.3 mHz) sine wave with a 2 dB amplitude impressed upon the 31 January 0714 UT data set. The 2 dB amplitude variation is based upon the likely effect a 5% depletion will cause in power variation (*Sales and Platt, 1989*). Comparing this figure to the original (Figure 8a) it can be seen that a 2 dB perturbation to the received signal amplitude is not clearly recognizable over the background noise. When the injected signal amplitude was raised to 6 dB the Fourier component became clearly recognizable and this can be seen in Figure 9b. Since a heating effect is unlikely to often cause a 6 dB variation in received power, amplitude observation of oblique heating with a 5 minute period during these sort of ionospheric conditions may prove to be difficult. During or near the period of future experiments it will therefore be useful to determine the spectral components of the background ionosphere and thus assess its effect on processing data. This will allow for the adjustment of the heater on/off cycle period during the experiment to place it into a clear region of the frequency spectrum. A strong data base of background ionospheric conditions during the experiment will also help during post processing to recognize and mitigate against the effects of natural irregularity structures.

## 6.2 Elevation Angle

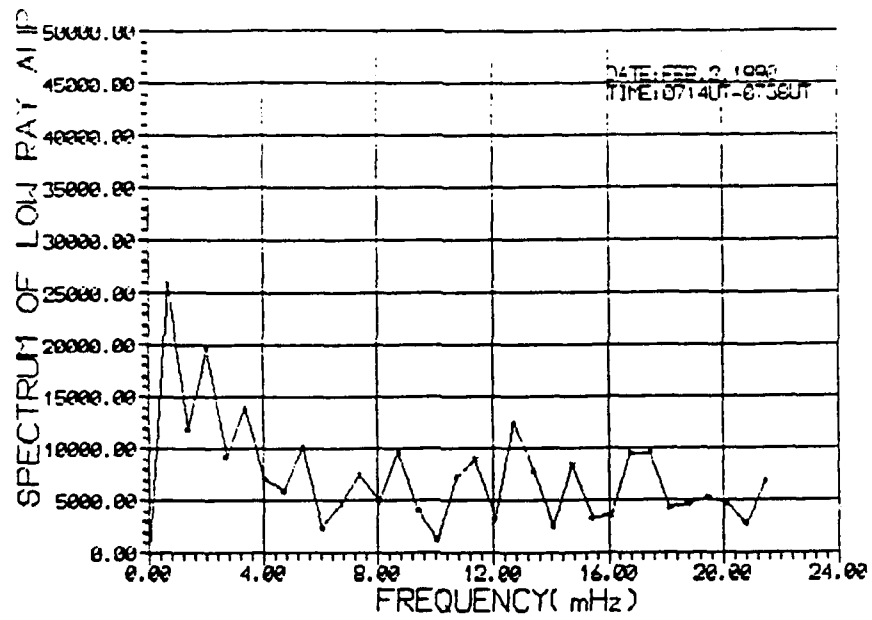
The plot of elevation angle versus time shown in Figure 10a, for the period 0427 - 0623 UT on January 31, appears to be highly structured. In particular there are a number of small linear sections of the data, most clearly observed around the 40 - 90 sample time mark. This appears similar (except for the period) to the structure often seen on backscatter radars and attributed

to the passage of gravity waves (*Sampson et al.*, 1990). It should further be noticed that towards the end of this sample period, between the sample times 230-280, (near the MUF) distinct periodic structure can be seen.

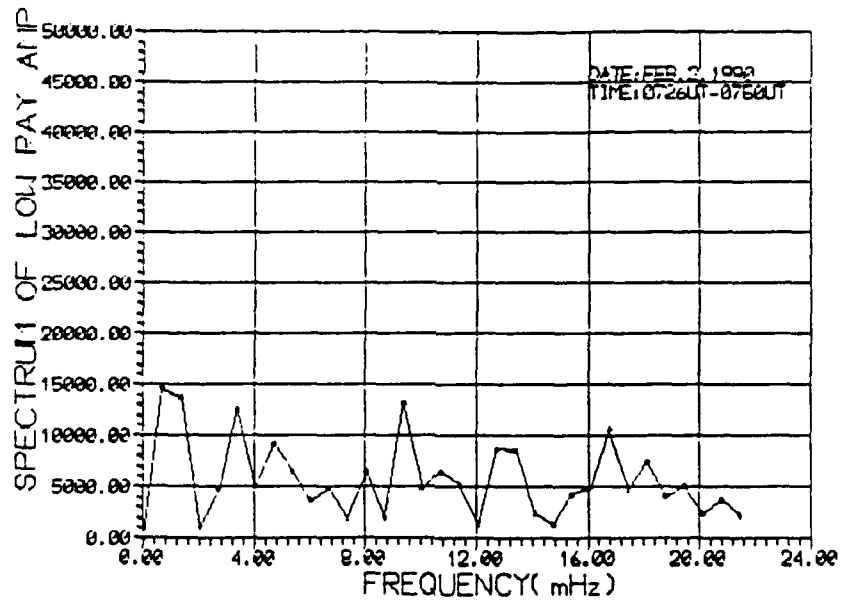
Figure 11 is a Fourier analysis of the whole sample period and shows no evidence of the above described structuring in the spectrum, thus indicating that it is not sufficiently periodic over the entire sample to be observed. Figure 12 is the spectral analysis for the 230-280 subset near the end of this period, and does show significant Fourier components in the frequency range 6.6 - 4.2 mHz (2.5 - 4 minute period). This effect results from both an enhanced spectral response of ionospheric structure in the 2.5 - 4 minute period and the longer period spectra being driven down due to the shorter sample time of the spectral analysis. The spectral power of Figure 12 is reduced from that of Figure 11 because of the smaller number of data points processed. The 2.5 - 4 minute periodic structure is difficult to explain in purely morphological terms (as is the other structure which does not Fourier analyze as periodic, but which never the less has some significant repetition). One explanation is that when more than two gravity waves at different angles occur the interference pattern can quickly become complicated resulting in shorter periods than one would normally expect from AGW's (10 minutes).

To test how well the 5 minute heater cycle could be detected in the Fourier analysis of the elevation angle an artificial cycle, assumed to be a 5 minute sine wave of amplitude  $2^\circ$ , was impressed upon the real data of the above time period. The result is shown in Figure 13a and as can be seen the induced heater signal is quite distinct in the spectra. If the elevation angle amplitude of the induced signal is reduced to  $0.6^\circ$  however, the 5 minute spectra (Figure 13b) is not easily distinguishable from the noise.

Figure 10b is a plot of elevation angle data for the time period 0714-0808 on February 2. In this time period, examples of the linear structure can also be seen. An unusual feature of this data sample is where the high ray and low ray appear to intersect at  $\sim 0725$  UT (sample time 28). From the plot of the MOF and heater frequency it can be seen that during this time the MOF dropped down to within a very close value of the heater frequency

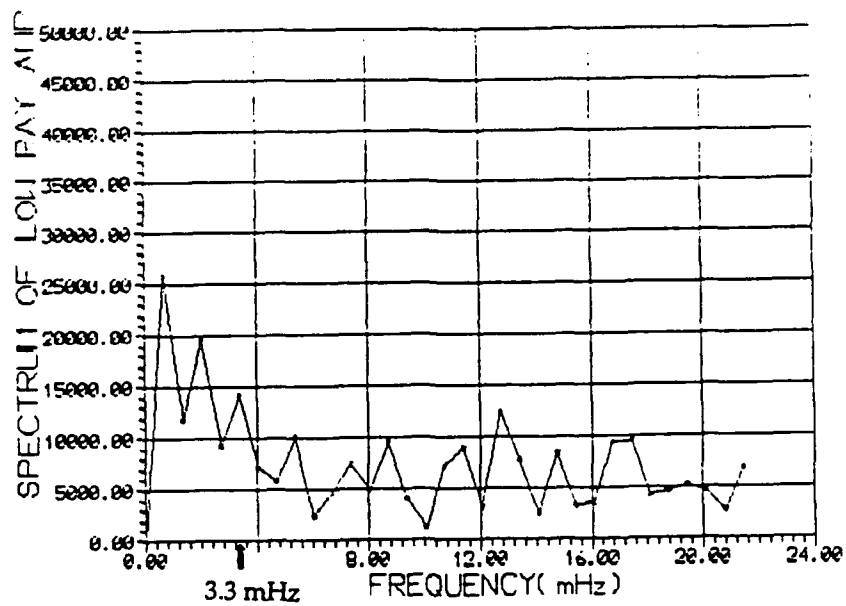


a)

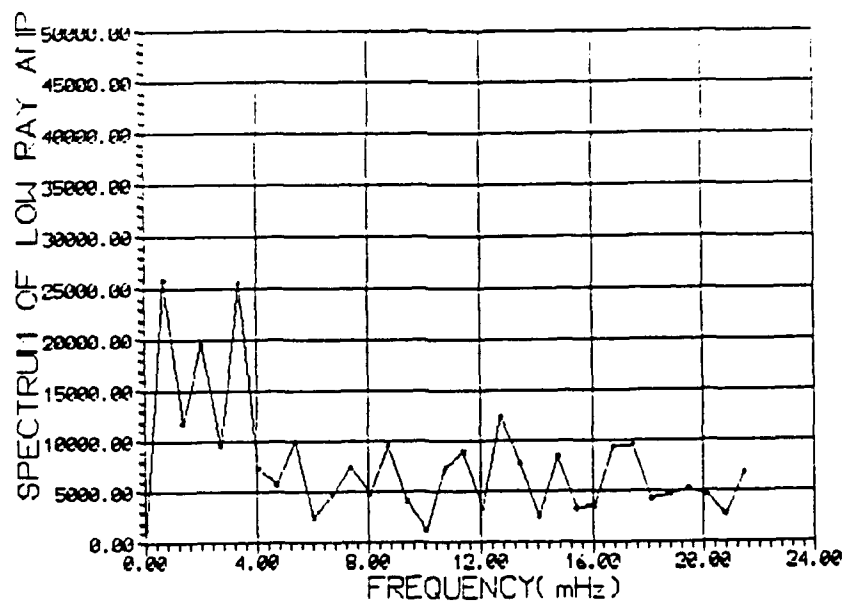


b)

Figure 8. Fourier spectra of the low ray amplitude variation for two 24 minute periods on 2 February starting at a) 0714 UT, b) 0726 UT



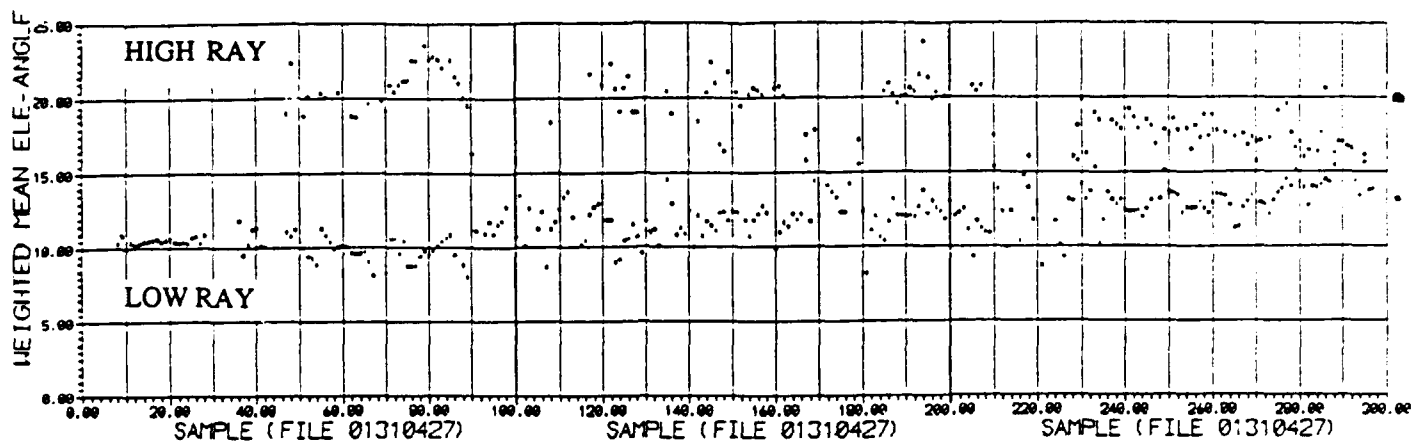
a)



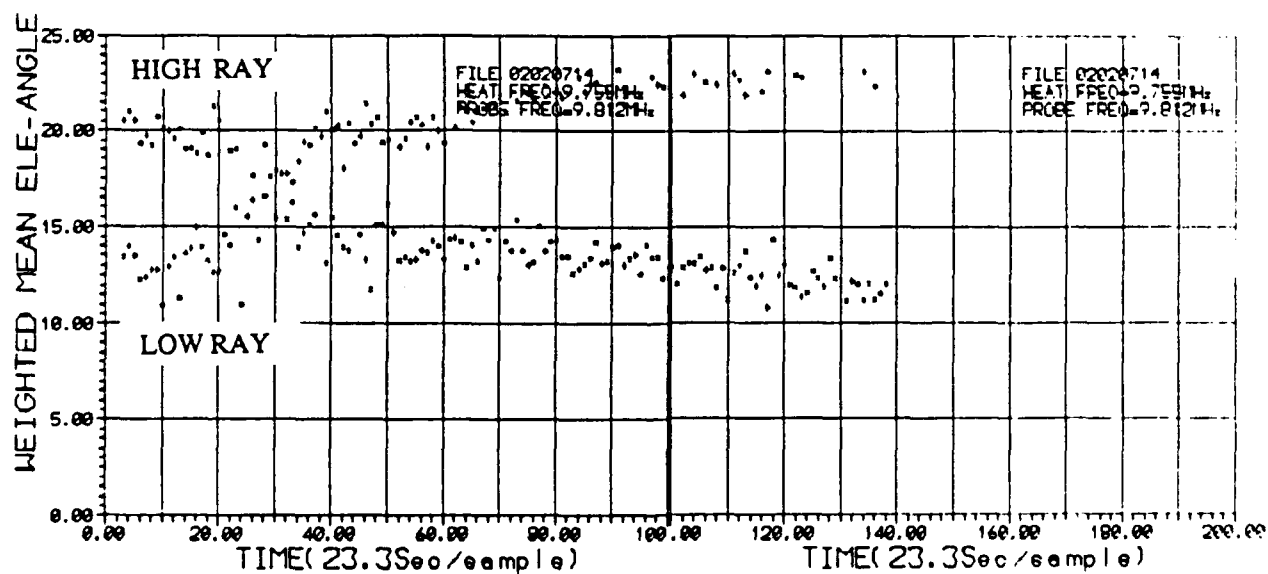
b)

Figure 9. Simulation of the 5 minute heater cycle amplitude by a sine wave injected into the data of 0714 UT on 2 February for a) 2 dB amplitude variation, b) 6 dB amplitude variation





a)



b)

Figure 10. Elevation angle of the low and high rays as a function of time for the periods a) 0427-0623 UT on 31 January, b) 0714-0808 on 2 February

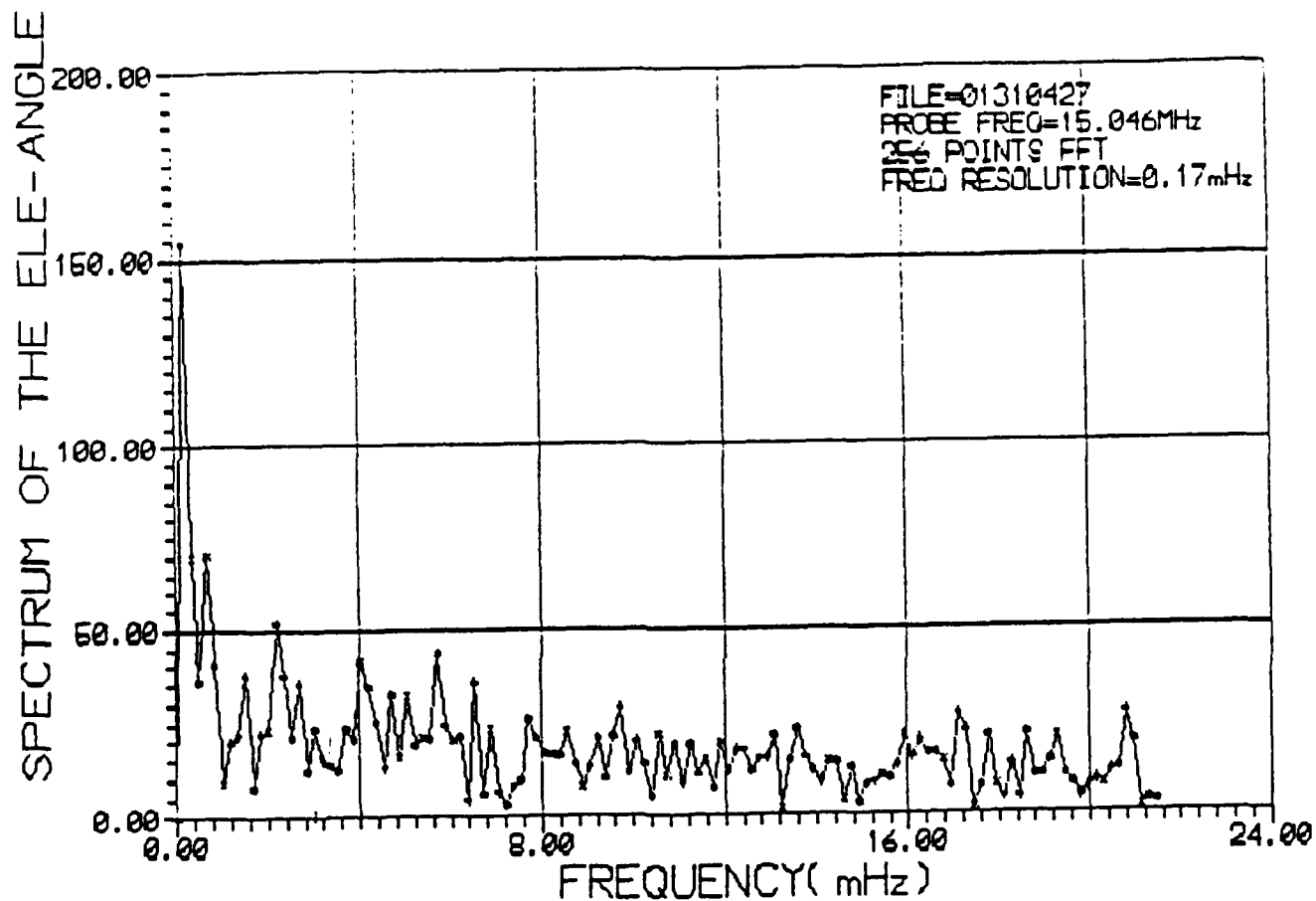


Figure 11. Fourier spectra of the ray elevation angle for the period 0427-0622 UT on 31 January

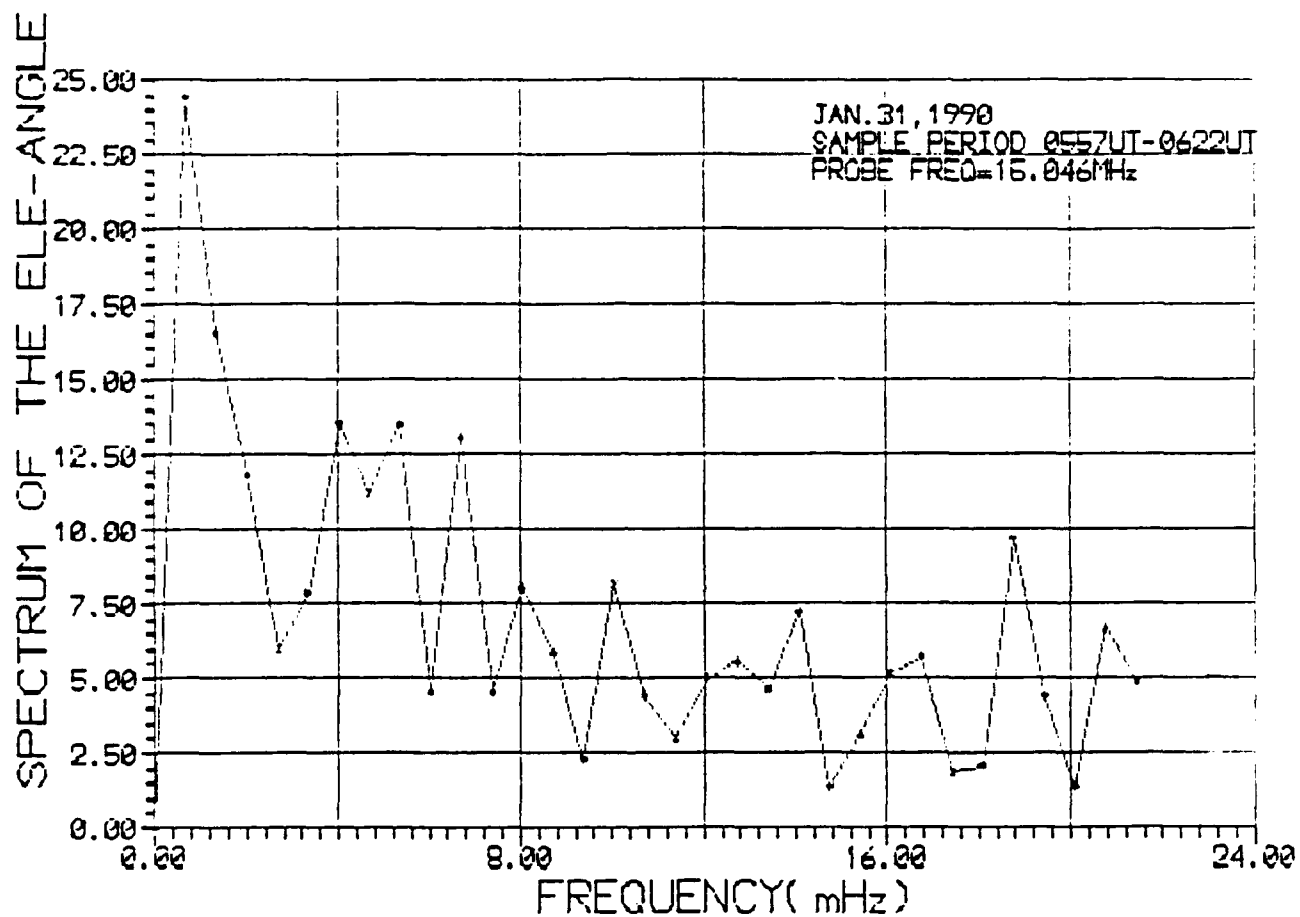
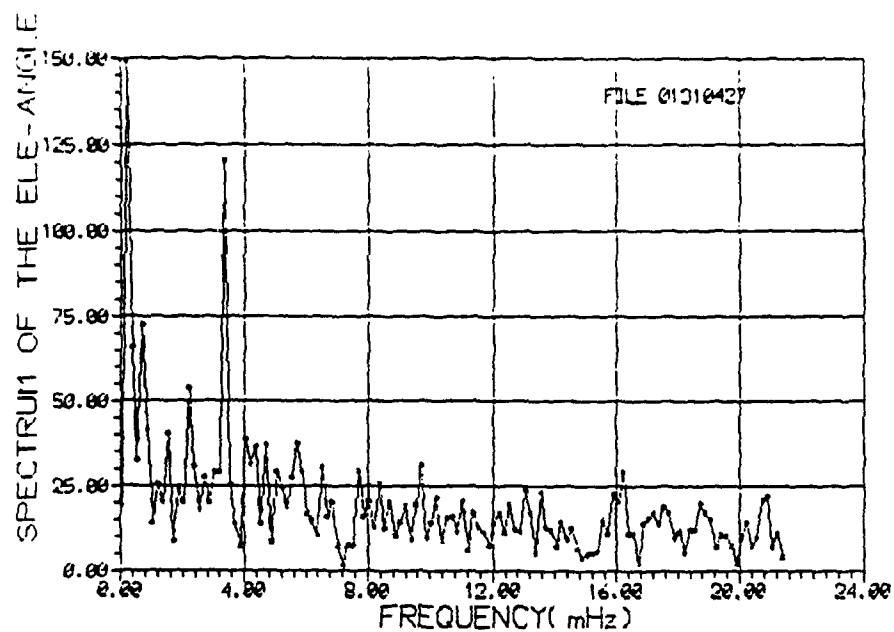
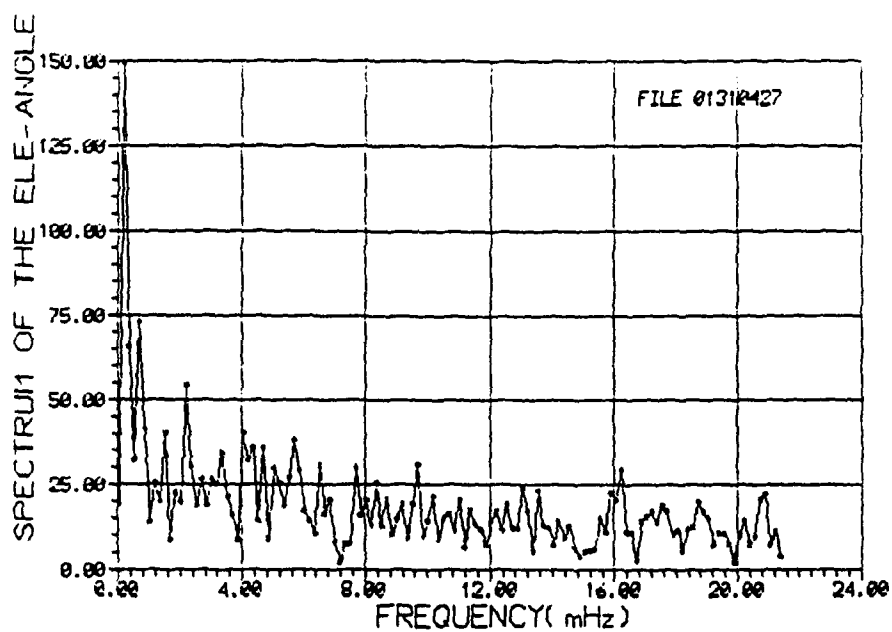


Figure 12. Fourier spectra of the low ray elevation angle for a subset (0557-0622 UT) of the data Figure 10a for 31 January 1990



a)



b)

Figure 13. Simulation of the 5 minute heater cycle change in elevation by using a sine wave injected into the data of 0427 UT on 31 January for a) a 2° elevation angle variation, b) 0.6° elevation angle variation

before starting to rise again. Here the high ray and low ray become nearly the same (the limit is where only one ray exists exactly at the skip).

### 6.3 Skymap Data

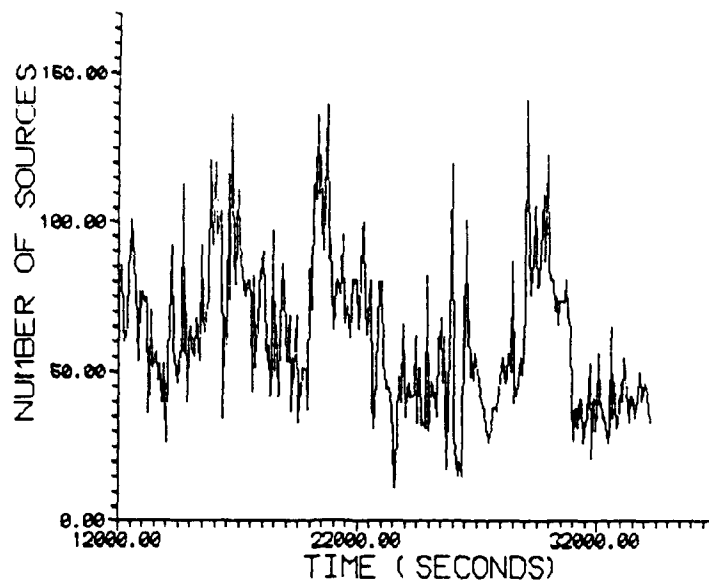
Figure 14 is a plot of the number of ionospheric reflection sources vs. time observed by the Digisonde at Kirtland in its drift mode. Figure 14a is for the period beginning at 0320 on 31 January while Figure 14b is for the period beginning at 0347 on 2 February. Clearly evident on both of these plots is the large variation in the number of sources over each observation period. Figure 14a in particular displays a regular rise and fall of the number of sources over time intervals of  $\sim 1$  hour. Such variation is also evident in the source plot of Figure 14b, with one event in particular producing a large number of reflection sources. The number of sources may rise and fall in this way due to the passage of large wavelike disturbances such as AGW's. Consider for example the series of skymaps shown in Figure 4. There are clearly a number of globular regions due to large scale "patches" of reflection in the ionosphere. Two possible reasons for the existence of such patches are apparent: AGW's (or other large scale wavelike irregularities) and discrete patches of heater enhanced irregularities. AGW produced clusters will be seen to last for a time consistent with their phase velocity (minimum of  $\sim 100$  m/s giving periods of  $> 10$  minutes), while those produced by the heater enhanced irregularities will have a five minute appearance cycle. A Fourier spectrum of the number of sources is shown in Figure 15 and indicates that the vast majority of the power falls at the low frequency end of the spectrum and that no obvious heating component is present. The lifetimes of the cluster regions observed on the sky map also indicate that they are of a duration consistent with large scale AGW's.

A possible reason for the absence of the high frequency components due to multiple AGW interference as described in Section 6.2 to explain the short period observations in the elevation angles, is that the reflection points observed are integrated over a large area of the ionosphere. If one large amplitude AGW exists with two or more smaller amplitude waves impressed upon it, the resulting interference pattern may be quite

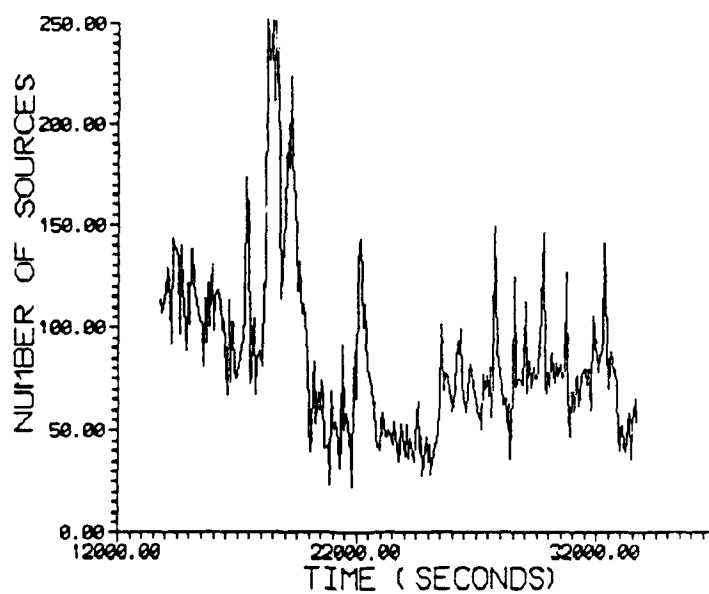
finely structured. Rays transmitted from the probe will then be subject to amplitude variations due to this fine structure. The Digisonde, however, integrates all these finer scale structures over the entire area and thus effectively does not see localized changes in their position. Only the very large scale changes in the ionosphere, such as the period of the dominant AGW will effect the total reflection source count. Further, since there are a large number of points in the Fourier analysis, the high frequency noise components will tend to be driven down. The relatively smooth spectra of ionospheric reflection sources means that the five minute growth decay cycle of the self-focussing instabilities should show up clearly in the spectra.

#### 6.4 Doppler Frequency

A plot of Doppler frequency line versus time is given in Figure 16 for the high ray and low ray during the period 0714 - 0808 UT on February 2. The Doppler value plotted for each CIT period is the power weighted mean of those Doppler lines which are determined to be low or high rays by the process described in Section 5.0. On this plot 10 Doppler lines correspond to 0.6 Hz of frequency shift, with 0 Hz at Doppler line 200. This example is for the same period already described in Section 6.2 where the MOF dropped down to near the heater frequency at ~ 0725 UT (sample time 28) and then began to rise again. At this point the Doppler lines of the low ray and high ray cross over. As the foF2 decreases and the ionosphere moves downward, both low and high ray have positive Doppler velocities. The high ray will usually have the greatest magnitude of Doppler velocity because of its greater phase retardation. As the ionosphere starts to move upwards again the Doppler velocity of both rays becomes more negative.



a)



b)

Figure 14. Number of ionospheric reflection sources versus time for the periods a) 0320-0930 UT on 31 January, b) 0347-0920 UT on 2 February

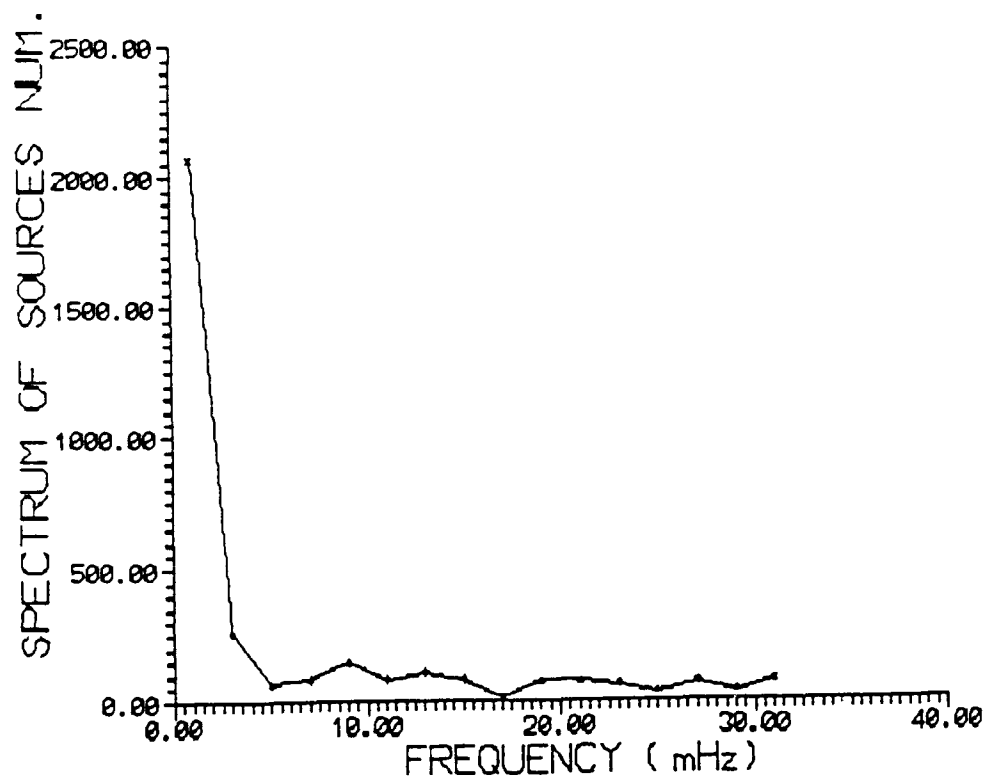


Figure 15. Fourier spectra of the number of source data observed by the Digisonde for the period 0320-0930 UT on 31 January



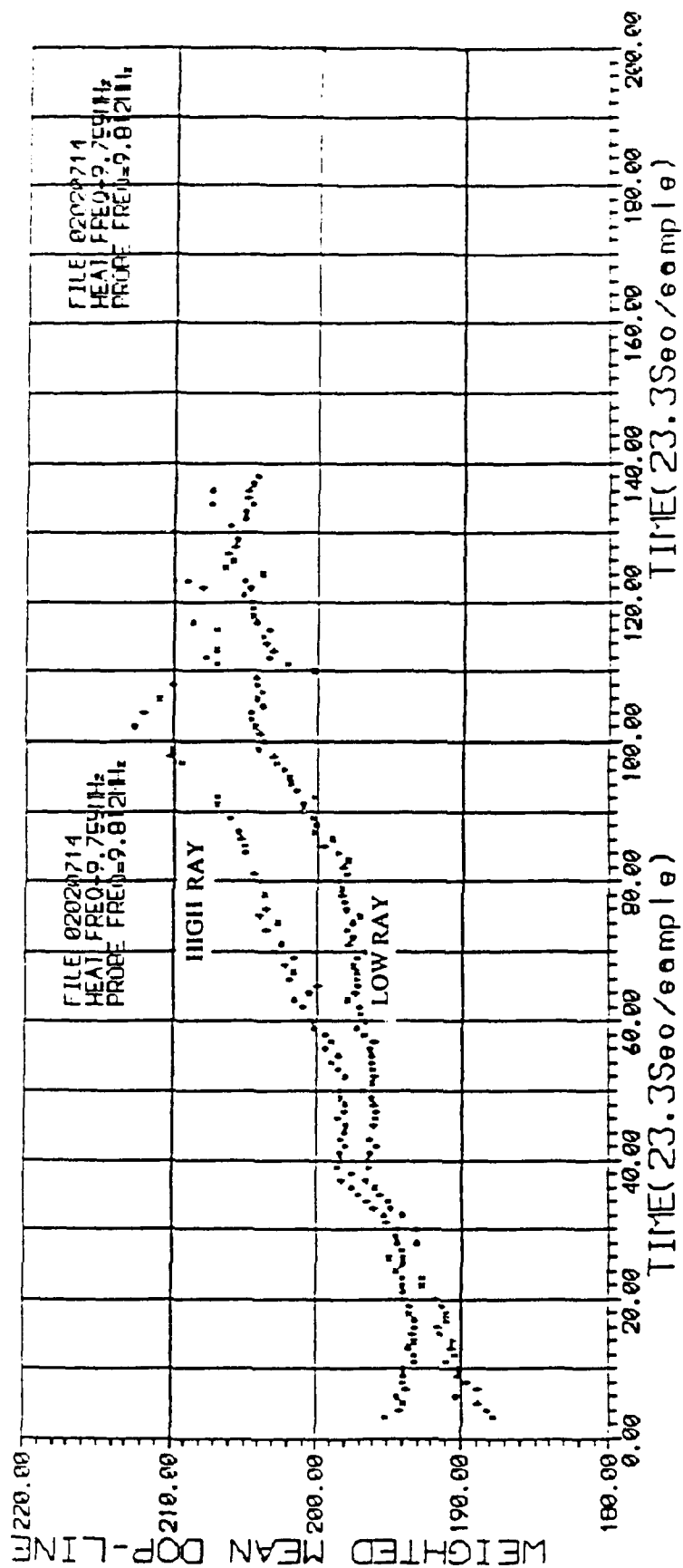


Figure 16. Doppler variation as a function of time for both the high and low ray for the period of 0714-0808 UT on 2 February

## 7.0 SUMMARY AND CONCLUSIONS

In all the data that was processed for the January/February campaign no unambiguous evidence of a heating effect was observed. This is was to be expected since the VOA transmitter was only operating on 375 kW instead of its full capability of 1.1 MW. Soviet research has indicated that 90 dBW of transmitted power can modify the ionosphere sufficiently to be observed. With just one of the three transmitter bays operating, VOA's effective radiated power is only  $\sim 86$  dBW. Future oblique heating experiments will be conducted with all three of VOA's transmitter bays operational, providing the required 90 dBW of transmitter power.

In general the operational procedure proved to be quite successful, though a number of improvements to the procedure became evident during the experiment. These include:

- 1) The calculation of VOA's Effective Radiated Power (ERP) should be conducted at intervals during the experiment. This is required to ensure that the VOA remains configured to transmit its maximum power into the heated region.
- 2) Direct observation of the VOA on/off cycle at the probe receiver site was not always possible. To improve this, the Doppler signature ( $-2$  Hz) of the VOA amplitude modulation could be used to clearly detect the on/off cycle.

It became clear during the experiment that the small number of discrete frequencies offered by VOA would lead to a reduction in the heating effect for much of the period, since the caustic region responsible for heating could not be placed as near to the F-peak as desirable. The small number of discrete frequencies meant that the next frequency below the MUF had to be chosen and the ionosphere allowed to decay through it. In many cases only half an hour of optimally placed data (i.e. operating frequency near the MUF) was available. This problem is not able to be overcome in the future, and shows the necessity for efficient frequency management.

In processing the elevation angle and amplitude data a number of major factors influencing the experimental results presented themselves:

- 1) The low period variations seen (most likely due to AGW's) can "spill out" into the spectrum considerably. For the period under discussion (January/February) the skymaps clearly indicate that large gravity wave structures were a common event during the experiment. Simulations indicate that the often large amount of natural ionospheric structure depositing power into the 5 minute region of the spectra may make the heater induced variations in elevation angle and amplitude difficult to detect. This highlights the need to assess the natural ionospheric conditions before the experiment and determine the optimum heater cycle. In fact the Fourier spectra of amplitude data for this experiment indicate that it may be beneficial to move the heater cycle time to between 2-3 minutes where less spectral background noise exists.
- 2) It is clear from the amplitude data that a great deal of intense and greatly variable high frequency fading (both in amplitude and time) occurs most likely due to O and X mode interference or micro mode interference. Since the CIT is 23.3 seconds, fading at frequencies greater than 25 mHz may be aliased back into the Doppler spectrum adding to the noise in the Fourier spectra around the main region of interest. In future experiments a CIT of 15 seconds can be chosen at intervals to unfold some of this short period fading and determine its aliasing effect on the data.

Because the ionospheric conditions over Kirtland consist of globular regions of reflection sources, the roughness model developed by *Sales et al.* (1990) for a more uniform ionospheric distribution of sources, cannot be used effectively. For the Kirtland type ionosphere the method would have to be modified to determine the center of each cluster and then the distribution of sources within each cluster. In this way the cluster regions, which likely correspond to the passage of large scale AGW's, can be tracked across the ionosphere with time and this in itself will give a good indication of the type and distribution of these irregularities. The distribution of reflection sources within each cluster will provide information about the

smaller scale density structure within it. It is quite possible that these globular regions will give the most suitable ionospheric conditions for the generation and observation of heater induced self-focussing irregularities, since the reflection geometry for the HF radar is obviously enhanced here and the gradients induced by the large structures will aid in achieving the threshold for instability processes.

## 8.0 REFERENCES

- Dozois, C. G., "A High Frequency Radio Technique for Measuring Plasma Drifts in the Ionosphere," *Scientific Report No. 6, AFGL-TR-83-0202, ULRF-424/CAR, ADA140509*, 1983.
- Gurevich, A. V., "Nonlinear Phenomena In the Ionosphere", *Springer Verlag*, New York City, 1978.
- Sales, G. S. and I. G. Platt, "High Power Oblique Incidence HF Ionospheric Modification," *GL-TR-90-0078*, April 1990, ADA224402.
- Sales, G. S., B. W. Reinisch and J. A. Ralls, "Techniques for Measuring Ionospheric Irregularities Generated by High Power Oblique HF Heating of the F-region," *Scientific Report No. 2, GL-TR-90-0206*, August 1990.
- Sampson, J. C., R. A. Greenwald, J. M. Ruohoniemi, A. Frey and K. B. Baker, "Goose Bay Radar Observations of Earth Reflected, Atmospheric Gravity Waves In the Ionosphere," *J. Geophys. Res.*, Vol. 95, pp. 7693-7709, 1990.